15. VACUUM SYSTEMS

The vacuum system for the proposed facility is readily achievable with conventional vacuum techniques, hardware, and established fabrication processes. Many of the difficult technical challenges associated with synchrotron light source storage rings (such as ALS, NSLS, etc.) are sidestepped by the relatively short beam lifetime of the recirculating linac. The short beam lifetime allows relatively high limits on background gas pressure. The one exception to this is in the region of the photocathode where vacuum pressures of 10^{-11} are often required to preserve cathode lifetimes. The low-average beam current also contributes to the simplification of the vacuum system design. As will be explained in more detail, the 10 – 30 μA beam current produces very little synchrotron radiation power loading on the vacuum chamber walls and thus the need for an *ante-chamber* (as used in ALS, PEP-II and other machines) is eliminated. With very modest limits on the gas pressure and minimal outgassing due to low levels of synchrotron radiation, the vacuum chamber dimensions can be adjusted to minimize the energy loss due to coherent synchrotron radiation (CSR) and resistive wall wakefield effects.

For significantly increased beam power levels, a more standard vacuum chamber with distributed ion pumps within the dipole magnets, and perhaps a separately pumped ante-chamber may be desirable. The proposed machine configuration does not preclude this as a potential upgrade.

The baseline electron beam current is 10 μA (1 nC/bunch at 10kHz) at an energy of 2.5 GeV. However, to allow for potential upgrades to the design, the vacuum system is designed for 30 μA at 3.1 GeV. The bunch length is compressed from 20 ps at the cathode to 2 ps at the exit of the arc connecting the pre-accelerator to the re-circulating linac (Arc 0). This bunch length is then held constant throughout the re-circulating sections. Note the term *Arc* as used throughout this chapters refers to entire circulation path at a given energy, straight sections as well as the curved sections at the ends of the straights.

The design of vacuum systems for synchrotron radiation sources must consider several physical processes in order to establish the allowable background gas partial pressures and chamber dimensions. These processes include:

- Beam loss due to interaction with background gas by
  - inelastic (Bremsstrahlung) scattering of the beam with residual gas nuclei and
  - large angle elastic (Coulomb) scattering of the beam with residual gas nuclei.
- Energy loss, resulting in longitudinal emittance growth due to coherent synchrotron radiation (CSR)
- Transverse emittance growth due to resistive wall wakefields

To reduce the energy loss resulting from CSR, the vacuum chamber aperture is reduced as reported in Chapter 4-Collective Effects. This has the effect of producing a higher cut-off frequency for the radiation propagating within the vacuum chamber. The coherent radiation emission process is then effectively suppressed. An upper limit on the vacuum chamber internal height (or equivalently the amount of CSR shielding required) is determined by allowed energy

loss. The CSR affect is present only in the bend magnets, and a larger beampipe aperture may be employed elsewhere.

The resistive wall wakefield is generated by the electron beam traveling in a vacuum chamber of finite conductivity. It is proportional to the chamber length and inversely proportional to both the square root of the chamber's electrical conductivity σ_c and the cube of the chamber's half-height, b. The resistive wall effect therefore has implications on the choice of vacuum chamber material, the minimum tolerable chamber height, and the location tolerance of the chamber with respect to the nominal beam axis.

The final chamber geometry, and most importantly the chamber inner height, will be determined by selecting an appropriate trade off between reducing the effects of CSR, resistive wall, and beam loss due to collisional scattering with the background gas. An example of this trade is the plot of the CSR energy loss and transverse resistive wall distortion as a function of chamber height shown in Figure 15-1. These affects are different for each beam pass as a result of the different beam energy and magnet bend radii. The optimal chamber height is therefore different for each arc. From an analysis of collective effects, as described in Chapter 4-Collective Effects, a minimum vacuum chamber height of 9 mm is indicated.

Since the actual values and effects of longitudinal emittance growth are still to be assessed, the beam chamber heights indicated in this report are preliminary.

BEAM LOSS DUE TO BEAM – GAS COLLISIONS

In contrast to storage rings, the 10μs time-of-flight (900 meter total path length) place extremely modest limitations on the allowable background gas pressure. We consider here in elastic and elastic scattering.

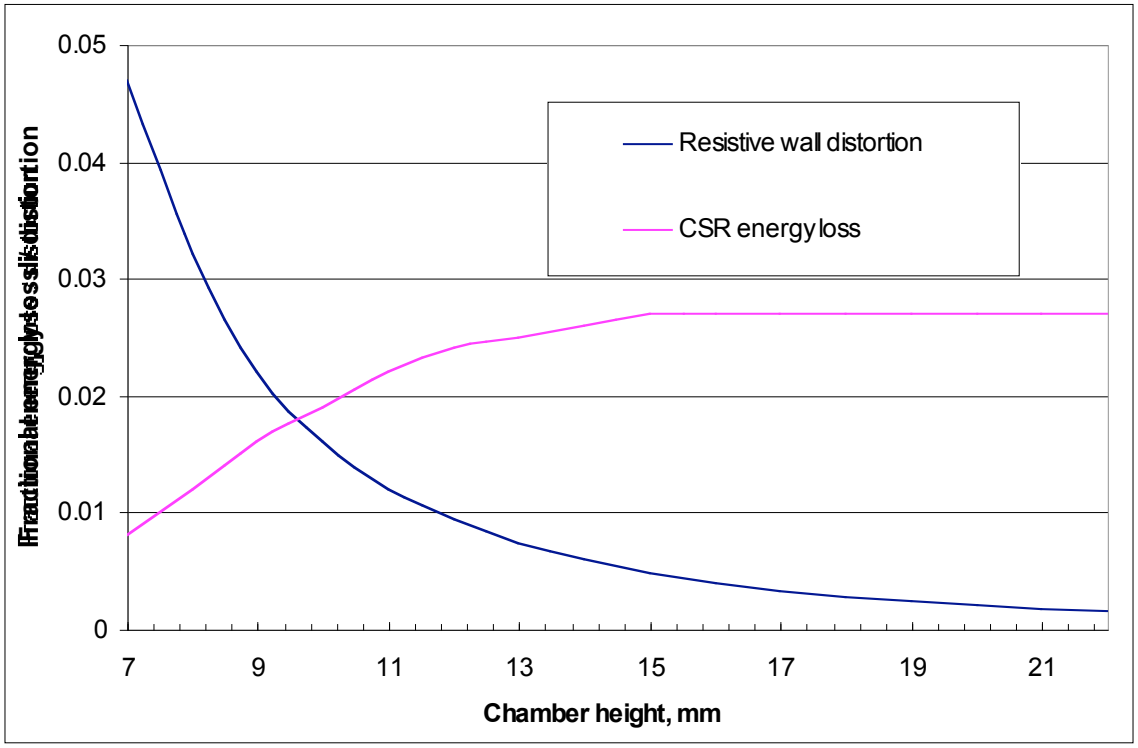

Figure 15-1 Comparison of fractional energy loss due to CSR and beam distortion from resistive wall effects as a function of chamber height.

Inelastic Scattering

Charged particles passing through matter become deflected by the strong electric fields of the nucleus. This deflection constitutes a transverse acceleration of the particle and results in a loss of energy through Bremsstrahlung radiation. If the energy loss exceeds the energy acceptance of the accelerator, δ_{acc}, (δ_{acc} = $\Delta E/E$) the particle is lost. For highly relativistic beams the probability for a particle to suffer a fractional energy loss of more than δ_{acc} per radiation length is [1],

$$P_r = \frac{4}{3}\ln(\delta_{acc}) \tag{1}$$

The probability of particle loss per unit time is equal to the beam decay rate or equal to the inverse of the bremsstrahlung lifetime,

$$\tau_{bs}^{-1} = \frac{4}{3}\frac{c}{L_r}\ln(1/\delta_{acc}) \tag{2}$$

where c is the speed of light and L_r is the radiation length. The radiation length for gas is a function of the partial pressure of each residual gas species. However, the composite atomic number of typical gas components in ultra high vacuum systems is roughly equivalent to

nitrogen. Therefore the radiation length for nitrogen (200 m at standard temperature and pressure (STP)), scaled appropriately for pressure, P_{vac} [nTorr], has been used to derive a simplified equation for bremstahlung lifetime, [1]

$$\tau_{bs}^{-1}\left[hr^{-1}\right] = 0.00653\, P_{vac} \ln\left(1/\eta_{acc}\right) \tag{3}$$

Assuming a conservative energy acceptance fraction of η_{acc} = 0.001, the bremsstrahlung lifetime for residual gas pressures from 10^{-4} to 10^{-8} Torr is 0.8 – 8,000 seconds. While admittedly short by storage ring standards, this is well in excess of recirculating linac requirements.

Elastic Scattering

An electron passing through background gas may also experience an elastic collision (Coulomb scattering) that causes an angular deflection large enough to give the particle a betatron oscillation amplitude larger than the limiting physical or dynamic aperture of the accelerator. For planning purposes, and to be consistent with the collective beam effects discussed above, a limiting physical rectangular aperture of 9 mm vertical and 40 mm horizontal has been assumed. In accordance with good machine design practice, we assume that the dynamic aperture will exceed the physical aperture throughout the accelerator. From Turner [2], the limiting aperture can be represented by the setting the admittance, A_x, where

$$A_x = a_x(s)^2 / \beta(s) \tag{4}$$

$a_x(s)$ is the limiting physical aperture and $\beta(s)$ is the local betatron function to

$$A_x = \beta_x \theta_{Ax}^2 \tag{5}$$

Since a loss rate for the accelerator as a whole is required, β_x may be taken to be the average betatron function over the arc sections and θ_{Ax} is the scattering angle corresponding to the limiting admittance. For the present study, an average betatron function of 30 m has been selected based on MAD output for the lattice as presently configured plus an additional 50%. A *worst-case* local betatron function of 90 m has been used based on the highest value found anywhere in the lattice for either *x* or *y*-axis. Similar equations can be formulated for the other transverse dimension. The beam lifetime, τ_{bg}, from Turner [3] for a rectangular aperture is;

$$\tau_{bg} = \left[nc \left(\frac{2\,(Z\, e_{cgs})^2}{pc} \right)^2 \left(\sqrt{\frac{\beta_x \beta_y}{A_x A_y}} + \frac{\beta_y}{A_y} \arctan\left(\sqrt{\frac{A_x \beta_y}{\beta_x A_y}} \right) + \frac{\beta_x}{A_x} \arctan\left(\sqrt{\frac{A_y \beta_x}{\beta_y A_x}} \right) \right) \right] \tag{6}$$

Note the dimensions of the quantities used in this equation are in gaussian units. The quantity Ze_{cgs} is the charge of the gas nucleus. As before, a nitrogen equivalent composite residual gas has been assumed. The beam energy term, *pc* (ergs), is the product of momentum

and the speed of light. The density of gas molecules, n, in molecules per cm^2, is directly proportional to the residual gas pressure at a given temperature. The fractional loss of beam for each beam energy level (re-circulation pass) is approximately,

$$\text{Beam loss fraction} = S / (\sigma_{bg}\, c) \tag{7}$$

where S is the path length of the beam. A plot of the fractional beam loss for each re-circulation pass over a range of residual gas pressures is shown in Figure 15-2.

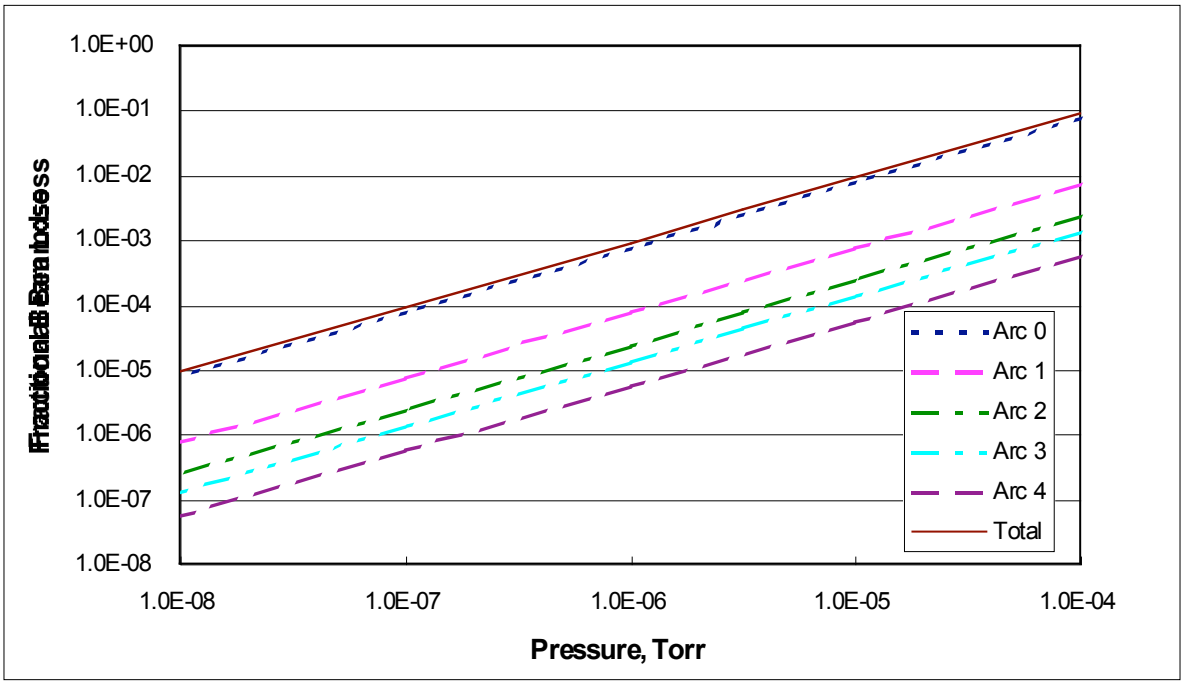

Figure 15-2 Beam loss fraction, due to Coulomb scattering, as a function of residual gas pressure.

The scattered beam will deposit energy on the vacuum chamber wall. This power deposition could lead to elevated wall temperatures and higher outgassing rates. The amount of scattered beam energy is a product of the fractional beam loss, the beam energy and the pulse frequency. On a per meter basis the power deposition, P_{scat}, is

$$P_{scat} = b_{rate}\, N_e \left(\frac{l}{\sigma_{bg}\, c}\right) E \tag{8}$$

where b_{rate} = bunch rate of 10^4 pulse/sec, and N_e = 1.87 x 10^{10}, number of electrons in a 3nC bunch,

Table 15-1 Line power density on vacuum chamber due to Coulomb scattering (W/m)

Pass \ Pressure	10^{-4} Torr	10^{-5} Torr	10^{-6} Torr	10^{-7} Torr	10^{-8} Torr
Arc 0	3.712	0.371	0.037	3.71E-03	3.71E-04
Arc 1	0.515	0.051	5.15E-03	5.15E-04	5.15E-05
Arc 2	0.277	0.028	2.77E-03	2.77E-04	2.77E-05
Arc 3	0.189	0.019	1.89E-03	1.89E-04	1.89E-05
Arc 4	0.144	0.014	1.44E-03	1.44E-04	1.44E-05

The results of these scattering calculations indicate that inelastic scattering is not a significant effect for the proposed geometry and fractional beam loss from elastic scattering will be less than 0.1% for residual gas pressures up to 2 x 10^{-6} Torr. As shown in Figure 15-1, most of the beam loss from elastic scattering occurs in the arc between the injector and linac (Arc 0). This suggests that the residual gas pressure limits should be different for the various re-circulation passes. Commensurate with the modest beam losses, the power deposition on the vacuum chamber is relatively insignificant for residual gas pressures as high as 10^{-5} Torr.

VACUUM SYSTEM LAYOUT

The vacuum system must accommodate the magnet lattice as well as the various collective beam effects. With the exception of the first arc and the spreader regions, the lattice consists primarily of identical dipole, quadrupole and sextupole magnets. In cross section these units are identical to the ALS booster ring magnets. Pole gaps in the dipoles are 30 mm (full height). The radial dimension to the pole tips of the quadrupoles and sextupoles are 32.5 and 35 mm, respectively. These magnets set the maximum external dimensions of the beam tube throughout the accelerator. Collective beam effects dictate the inner height of the beam tube (vacuum chamber) within bend magnets.

The residual gas pressure requirements appear to be very modest. For design purposes a conservative upper limit on the average gas pressure of 1 x 10^{-6} Torr will be used. As with any vacuum system, the pressure is determined by the amount of gas introduced, the conductance of the gas to the pumps and the pump speed. The gas load is a product of thermal outgassing and photon induced desorption.

The amount and mixture of gas liberated from the vacuum wall is a function of the material selected and its preparation. Aluminum is the primary candidate for the vacuum tube because it is relatively inexpensive to extrude, has good vacuum properties, is compatible with commercially available UHV fittings, has adequate electrical conductivity, and has a good track record in other synchrotron light sources. For the purposes of this study, a vacuum baked (150°C for 24 hrs.) aluminum beam tube and "conflat" type metal sealed fittings are assumed.

The vacuum system presented here consists of an extruded rectangular beam tube in the bend magnet locations transitioning to a circular tube in the straight sections. The external height of the rectangular beam tube is 1 to 2 mm smaller than the magnet pole tip gap. The internal height

of the rectangular tube varies with each arc as determined by collective effects described previously; 9 mm in Arc 0, 12.8 mm in Arc 1, 16.9 mm in Arc 2, 20 mm in Arc 3, 20.9 mm in Arc 4. The beam tube is connected periodically to a large diameter aluminum pipe that serves as a pumping manifold. A series of modular cryosorption pumps are distributed along the manifold to provide the primary pumping. A small number of turbomolecular pumps backed by oil-free roughing pumps will provide the initial system vacuum. The roughing pumps will also provide pumping for cryopump regeneration, see Figures 15-3, 15-4.

While admittedly a distributed cryopumped system is not typical for storage ring synchrotron light sources, it is widely used in other large accelerators. The advantage of this type of system is that all of the components are readily available commercially. Secondly, the beam tube has a very simple, regular cross section that facilitates close tolerance extrusion. And, third, repair or replacement of the primary pumps can be performed without bringing any portion of the beam tube *up to air*.

The proposed system contains several variables that can be optimized based on the conditions within a given region of the accelerator. These variables include the width of the beam tube, spacing between manifold-beam tube connections, manifold diameter and cryopump spacing. While each portion of the accelerator section will behave differently, of primary concern are the bend magnets where gas production is the greatest and gas conductance is the least.

Synchrotron radiation induced outgassing.

The equations derived by Mathewson, *et al.* [3] are used in the following section to calculate outgassing rates due to synchrotron radiation. Gas is desorbed from the beam tube surface by thermal desorption and by photoelectrons that are generated by incident synchrotron radiation. The energy and quantity of the synchrotron radiation is a function of the photon critical energy. The critical energy, ε_c, of the photon is a function of the beam energy and the bending radius:

$$\varepsilon_c = 2.2\ 10^3 \frac{E^3}{\rho} \tag{9}$$

where the photon energy ε_c is in keV, the beam energy E is in GeV and ρ is the bend radius in m. The total photoelectron flux, η, at normal incidence per mA of beam is approximated by

$$\eta = 1.51 \times 10^{14} \frac{\rho E^{2/3}}{E^2} \left[2.61 \int_{10}^{1560} \varepsilon^{-2/3} \varepsilon^{-0.94}\, d\varepsilon + 441.9 \int_{1560}^{\varepsilon_c} \varepsilon^{-2/3} \varepsilon^{-1.13}\, d\varepsilon \right] \tag{10}$$

where E is the beam energy in GeV, and ρ is the magnetic bend radius in meters. For critical energies below 1560 eV the second integral is not valid and the term is dropped. Photons with energies below 10 eV do not generate photoelectrons in aluminum. The angle of incidence of the photons on the vacuum tube wall will be in the range of 5 to 13 degrees. A worst-case assumption of a $(1/\sin\theta)$ dependence has been used. The number of photoelectrons produced per meter of vacuum chamber, N_{pe}, (arc sections only) is obtained by multiplying the flux η by the

(1/ sin□) term and beam current, I (0.03 mA), and dividing by the equivalent length of chamber, L_{arc}, receiving the radiation.

$$N_{pe} = \frac{\square I}{2 L_{arc} \sin(\square)} \tag{11}$$

The angle of incidence, □, is a function of the beam tube width *w* and bend radius given by:

$$\square = cos^{-1}\left(\frac{\square}{\square + \frac{w}{2}}\right) \tag{12}$$

The results are summarized in Table 15-2.

Table 15-2 Photoelectron yield per meter for a 6 cm wide aluminum beam tube.

Location	□, eV	□	□, m	L_{arc}, m	□, deg	N_{pe}, 1/(m-sec)
Arc 0	3	0	1.20	3.6	12.68	0
Arc 1	619	3.3×10^{16}	2.30	9	9.20	3.4×10^{14}
Arc 2	2000	5.5×10^{16}	4.59	18	6.53	4.0×10^{14}
Arc 3	4176	9.1×10^{16}	6.88	27	5.34	5.4×10^{14}
Arc 4	7720	11.2×10^{16}	8.49	34	4.81	5.9×10^{14}

Gas is desorbed from the beam tube surface by the impingement of photoelectrons. For vacuum baked aluminum the desorption efficiency, □ (molecules/electron), is roughly equal to 0.1 – 0.15 [3,4]. In typical synchrotron light sources this value is reduced by many orders of magnitude through beam scrubbing. However the required circulating currents and durations (~ 10^6 mA-hours) are far in excess of re-circulating linac capabilities. The amount of gas desorbed by the beam due to photoelectrons is,

$$Q_{pe}[(\text{Torr-l/s}) / \text{m}] = 2 \square \square K \tag{13}$$

where K^{-1} is equal to the number of molecules per Torr-liter of gas at room temperature ($K = 3.03 \times 10^{-20}$). The factor of 2 is included because gas molecules are desorbed as the photoelectron leaves one surface and arrives at another. The efficiency of gas evolution by electron bombardment of aluminum peaks at electron energies of about 400 eV and then falls asymptotically to a relatively constant value above 2 keV [4]. Rough average values for □ over the 0.1 – 7 keV range were selected, as shown in Table 15-3. Calculated gas desorption rates, using these species specific □ values, are also shown in this table.

The power deposition on the vacuum tube wall from synchrotron radiation is a possible source of heating and therefore enhanced thermal desorption. The amount of synchrotron power, estimated from emission of an electron beam in uniform circular motion [5], results in a peak linear power density, 5.4 x 10^{-3} W/cm. Under worst-case assumptions [6], this power is deposited over a width of 0.24 mm resulting in a peak heat flux of only 0.5 W/cm^2. This level of localized heating is negligible for a reasonably thick aluminum beam tube and will not result in increased thermal outgassing.

Table 15-3 Photoelectron desorption efficiency and gas desorption rates per meter of beam tube by gas species.

□		Q_{pe} (Torr-liter/sec-m)				
Gas	h	Arc 0	Arc 1	Arc 2	Arc 3	Arc 4
Hydrogen	0.1	-	1.9 x 10^{-6}	2.3 x 10^{-6}	3.1 x 10^{-6}	3.3 x 10^{-6}
CO	0.03	-	5.8 x 10^{-7}	6.8 x 10^{-7}	9.2 x 10^{-7}	1.0 x 10^{-6}
CO2	0.025	-	4.8 x 10^{-7}	5.7 x 10^{-7}	7.6 x 10^{-7}	8.3 x 10^{-7}
Methane	0.008	-	1.5 x 10^{-7}	1.8 x 10^{-7}	2.4 x 10^{-7}	2.7 x 10^{-7}
Total			3.1 x 10^{-6}	3.7 x 10^{-6}	5.0 x 10^{-6}	5.4 x 10^{-6}

Thermally induced outgassing.

The quantity and composition of thermally desorbed gas is substantially altered by a moderate vacuum bake-out in aluminum systems, as shown in Table 15-4. Water is the dominant species in unbaked aluminum whereas hydrogen is most prolific in baked aluminum systems.

Table 15-4 Outgassing rates measured for an aluminum vacuum chamber after 100 hrs of pumping from [4] as shown in [2].

	Q (Torr-liters/sec-cm^2)	
Gas	Unbaked	Baked*
Hydrogen	7 x 10^{-12}	5 x 10^{-13}
Methane	5 x 10^{-13}	5 x 10^{-15}
Water	3 x 10^{-10}	< 1 x 10^{-15}□□□□□
Carbon monoxide	5 x 10^{-12}	1 x 10^{-14}
Carbon dioxide	5 x 10^{-13}	1 x 10^{-14}
*150°C for 24 hours		

All metal surfaces, including the beam tube, manifold and connecting tubulation are assumed to be clean, baked aluminum. The amount of thermal outgassing is the product of the rates shown in Table 15-4 and the surface area. For the beam tube of Arc 4 (2.1 cm x 6 cm) the gas produced per meter is 8.5 x 10^{-10} Torr-liter/sec or 6,000 times smaller than synchrotron radiation induced desorption.

Gas Pressure Profile

The most difficult pumping conditions are present in the arc sections due to the limited gas conductance and the synchrotron radiation induced gas load. The pumping of the straight sections is relatively straightforward in comparison and is not considered in this study. Given the assumption of a discretely pumped system, a rational configuration would include widely spaced pumps, a manifold sized to be consistent with the pump size and a limited number of beam tube penetrations. A system that meets the criteria consists of CTI-8 cryopumps centrally located on a 10 meter span of 20 cm diameter manifold. Short, 30 cm long by 5 cm diameter tube and bellows assemblies connect the manifold to the beam tube. An illustration of the vacuum system concept, as applied to Arc 4, is shown in Figure 15-3. A representative section of the system is shown schematically in Figure 15-4. Note that a single cryopump services a segment of Arc 4 containing 9 dipole magnets.

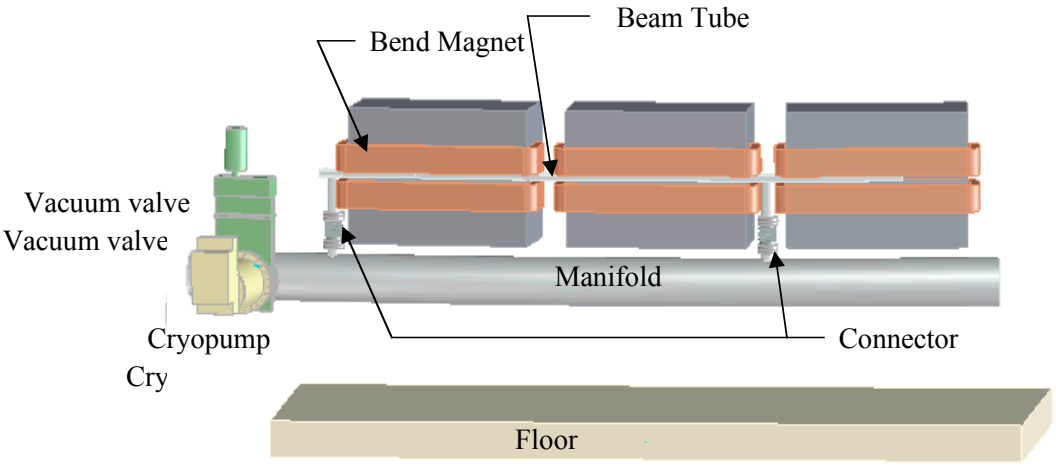

Figure 15-3 Conceptual layout of a representative section of the vacuum system.

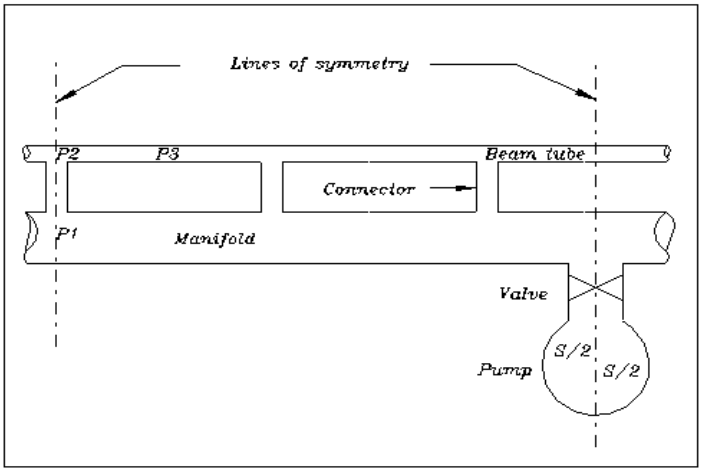

Figure 15-4 Schematic of a typical vacuum system section.

In addition to the outgassing rate, the pressure in the beam tube is a function of the gas conductance and pump speed. For ease of computation, gas evolved from the beam tube, connector tubing and manifold is treated as a single continuous distributed source along the length of the manifold. Using this assumption, the peak pressure in the manifold, P1, is given by:

$$\mathrm{P1} = Q\,L\left(\frac{1}{2\,C_L}\,\frac{1}{S_p}\right) + P_{base} \tag{14}$$

where Q is the outgassing rate in Torr-liters/sec per meter of beam tube,
C_L is the conductance of the manifold (from P1 to pump) in liters/sec,
S_p is the pumping speed (half of the full pump speed) in liters/sec,
L is half of the span between pumps in meters, and
P_{base} is the base pressure of the pump in Torr.

The conductance of the cylindrical tubing was calculated using Santeler's [7] correction to the common formula for a circular tube in molecular flow. Assuming the tube terminates into a larger volume, the manifold's conductance is from 1000 to 5000 liters/sec, depending on the gas species.

The pressure at the connecting tube entrance, P2, is determined by adding the pressure differential from gas flow through the connecting tube to the maximum pressure in the manifold, P1. The peak pressure in the beam tube, P3, is found by adding the maximum pressure increase along the beam tube, between connectors, to the pressure at the connector entrance, P2.

The conductance of the beam tube, C_{tube} [liter/s], is calculated using the equation from Roth [8] for a long rectangular tube of uniform cross section,

$$C_{tube} = \frac{8}{3}\sqrt{\frac{k\,T_g}{2\,\pi\,m}}\;1000\left(\frac{w^2\,b^2}{(w+b)\,L_r}\,K_c\right) \tag{15}$$

where k is the Boltzmann constant, 1.385×10^{-23} J/K,
T_g is the gas temperature in K,
m is the mass of the molecule in kg,
L_r is the half-span between connectors ($L_r = L_{\mathrm{tube}}$)
b is the full internal height of the beam tube,
w is the internal width of the beam tube, and
K_c is a constant that is a function of b/w (1.2 for present case).

The partial pressures in Arc 4 at P1 – P3 for the four dominant gas species are shown in Table 15-5. The base pressure of the cryopump is assumed to be 10^{-9} Torr, divided evenly between gas species. Actual base pressure of a properly maintained pump should be lower. All other arcs produce lower background pressure because the lower synchrotron radiation induced outgassing more than compensates for the reduced gas conductance.

Table 15-5 Partial pressures at key points (see Fig. 15-4) in the vacuum system.

	Sp (= S/2), l/s	P1, Torr	P2, Torr	P3, Torr
Hydrogen	1250	2.7×10^{-8}	7.5×10^{-8}	1.26×10^{-7}
CO	750	2.2×10^{-8}	7.5×10^{-8}	1.32×10^{-7}
CO_2	1250	1.9×10^{-8}	7.5×10^{-8}	1.34×10^{-7}
Methane	950	0.5×10^{-8}	1.6×10^{-8}	0.28×10^{-7}
Total	-	7.3×10^{-8}	2.4×10^{-8}	4.20×10^{-7}

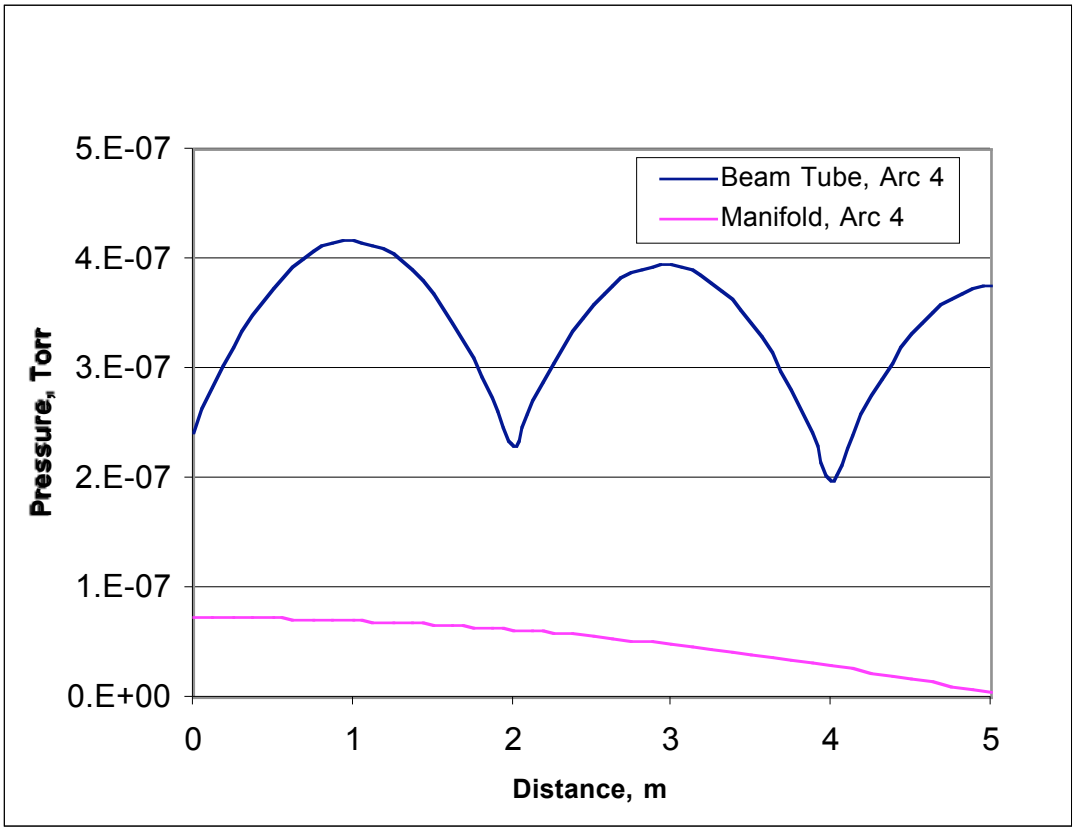

Figure 15-5 Pressure profile along a representative portion of the Arc 4 beam tube

The plot shown in Figure 15-5 is an approximate pressure profile of the Arc 4 beam tube derived by applying the methodology used to find pressures P1-P3 to the other analogous positions along the beam tube and then applying a parabolic profile between them. By inspection, the average pressure along the path of the beam is 3×10^{-7} Torr. This average residual gas pressure compares favorably with the 1×10^{-6} Torr design limit.

REFERENCES

[1] H. Wiedemann, *Particle Accelerator Physics* I-Basic Principles and Linear Beam Dynamics, Springer-Verlag, Berlin, pp.378-380, 1999

[2] W. C. Turner, *Notes for a Course on Accelerator Vacuum Physics*, CBP Tech. Note 188, June 11, 1999.

[3] A. G. Mathewson, G.H. Horikoshi, and H. Mizuno, *Some Notes on the Photoelectron Induced Gas Desorption Problems in the Photon Factor and Trist*an, National Lab for High Energy Physics Report, Japan.

[4] M. Achard, *Electron and Ion Induced Gas Desorption from Stainless Steel*, OFHC Copper, Titanium and Pure Aluminum, CERN-ISR-VA/76-34

[5] M. Sands 1970 (from PEP-II Conceptual Design Report)

[6] *PEP-II Conceptual Design Report*, June 1993, p. 305.

[7] D. J. Santeler, New Concepts in Molecular Gas Flow, J.Vac. Sci. Technol. A, Vol. 4, No. 3, May/June 1986

[8] Roth, *Vacuum Technology 2nd Ed.*, North-Holland, 1982 pp. 84-87.